Histidine-40 of ribonuclease T1 acts as base catalyst when the true catalytic base, glutamic acid-58, is replaced by alanine

ARTICLE *in* BIOCHEMISTRY · SEPTEMBER 1990

Impact Factor: 3.02 · Source: PubMed

4 AUTHORS, INCLUDING:

Jan Steyaert
Vrije Universiteit Brussel
136 PUBLICATIONS **4,718** CITATIONS

SEE PROFILE

Klaas Hallenga
University of Wisconsin–Madison
61 PUBLICATIONS **2,476** CITATIONS

SEE PROFILE

Lode Wyns
Vrije Universiteit Brussel
259 PUBLICATIONS **9,709** CITATIONS

SEE PROFILE

Schweitzer, D., Hausser, K. H., Taglieber, V., & Staab, H. A. (1976) *Chem. Phys. 14*, 183-187.
Sheldrick, G. M., Guy, J. J., Kennard, O., Rivera, V., & Waring, M. J. (1984) *J. Chem. Soc., Perkin Trans. 2 43*, 1601-1605.
Strum, J. (1982) *Biopolymers 21*, 1189-1206.
Suga, K., & Kinoshita, M. (1982) *Bull. Chem. Soc. Jpn. 55*, 1695-1704.
Tsao, D. H. H., Casas-Finet, J. R., Maki, A. H., & Chase, J. W. (1989) *Biophys. J. 55*, 927-936.
Ughetto, G., Wang, A. H.-J., Quigley, G. J., van der Marel, G. A., van Boom, J. H., & Rich, A. (1985) *Nucleic Acids Res. 13*, 2305-2323.
van der Waals, J. H., & de Groot, M. S. (1967) Magnetic Interactions Related to Phosphorescence, in *The Triplet State* (Zahlan, A. B., Ed.) pp 101-132, Cambridge University Press, Cambridge, England.
Van Dyke, M. M., & Dervan, P. B. (1984) *Science 225*, 1122-1127.
von Schütz, J. U., Zuclich, J., & Maki, A. H. (1974) *J. Am. Chem. Soc. 96*, 714-718.
Wakelin, L. P. G., & Waring, M. J. (1976) *Biochem. J. 157*, 721-740.
Wang, A. H.-J., Ughetto, G., Quigley, G. J., Hakoshima, T., van der Marel, G. A., van Boom, J. H., & Rich, A. (1984) *Science 225*, 1115-1121.
Ward, D. C., Reich, E., & Goldberg, I. H. (1965) *Science 149*, 1259-1264.
Waring, M. J., & Wakelin, L. P. G. (1974) *Nature 252*, 653-659.
Williamson, R. L., & Kwiram, A. L. (1988) *J. Chem. Phys. 88*, 6092-6106.
Wilson, W. D., Wang, Y.-H., Krishnamoorthy, C. R., & Smith, J. C. (1985) *Biochemistry 24*, 3991-3999.
Zang, L.-H., Maki, A. H., Murphy, J. B., & Chase, J. W. (1987) *Biophys. J. 52*, 867-872.
Zhou, N., James, T. L., & Shafer, R. H. (1989) *Biochemistry 28*, 5231-5239.

Histidine-40 of Ribonuclease T_1 Acts as Base Catalyst When the True Catalytic Base, Glutamic Acid-58, Is Replaced by Alanine†

Jan Steyaert,*,‡,§ Klaas Hallenga,‡ Lode Wyns,§ and Patrick Stanssens‡

Plant Genetic Systems NV, J. Plateaustraat 22, B-9000 Gent, Belgium, and Vrije Universiteit Brussel, Instituut Moleculaire Biologie, Paardestraat 65, B-1640 St-Genesius-Rode, Belgium

Received March 16, 1990; Revised Manuscript Received May 16, 1990

ABSTRACT: Mechanisms for the ribonuclease T_1 (RNase T_1; EC 3.1.27.3) catalyzed transesterification reaction generally include the proposal that Glu58 and His92 provide general base and general acid assistance, respectively [Heinemann, U., & Saenger, W. (1982) *Nature (London) 299*, 27-31]. This view was recently challenged by the observation that mutants substituted at position 58 retain high residual activity; a revised mechanism was proposed in which His40, and not Glu58, is engaged in catalysis as general base [Nishikawa, S., Morioka, H., Kim, H., Fuchimura, K., Tanaka, T., Uesugi, S., Hakoshima, T., Tomita, K., Ohtsuka, E., & Ikehara, M. (1987) *Biochemistry 26*, 8620-8624]. To clarify the functional roles of His40, Glu58, and His92, we analyzed the consequences of several amino acid substitutions (His40Ala, His40Lys, His40Asp, Glu58Ala, Glu58Gln, and His92Gln) on the kinetics of GpC transesterification. The dominant effect of all mutations is on k_{cat}, implicating His40, Glu58, and His92 in catalysis rather than in substrate binding. Plots of log (k_{cat}/K_m) vs pH for wild-type, His40Lys, and Glu58Ala RNase T_1, together with the NMR-determined pK_a values of the histidines of these enzymes, strongly support the view that Glu58-His92 acts as the base-acid couple. The curves also show that His40 is required in its protonated form for optimal activity of wild-type enzyme. We propose that the charged His40 participates in electrostatic stabilization of the transition state; the magnitude of the catalytic defect (a factor of 2000) from the His40 to Ala replacement suggests that electrostatic catalysis contributes considerably to the overall rate acceleration. For Glu58Ala RNase T_1, the pH dependence of the catalytic parameters suggests an altered mechanism in which His40 and His92 act as base and acid catalyst, respectively. The ability of His40 to adopt the function of general base must account for the significant activity remaining in Glu58-mutated enzymes.

Ribonuclease T_1 (RNase T_1, EC 3.1.27.3) from the fungus *Aspergillus oryzae* is the best known representative of a family of microbial ribonucleases sharing homology at both the sequence and structural level. The enzyme consists of a single polypeptide chain of 104 residues of known sequence and contains 2 disulfide bridges (Takahashi, 1971, 1985). The three-dimensional structure of RNase T_1, complexed with the competitive inhibitor guanosine 2'-phosphate (2'-GMP),[1] has been determined to 1.9-Å resolution by Heinemann and Saenger [1982; see also Arni et al. (1988) and Sugio et al.

† This work was supported by Plant Genetic Systems NV. J.S. is a Research Assistant of the Belgian National Fund for Scientific Research.
* Address correspondence to this author at the Vrije Universiteit Brussel.
‡ Plant Genetic Systems NV.
§ Vrije Universiteit Brussel.

[1] Abbreviations: barnase, *Bacillus amyloliquefaciens* ribonuclease; cGMP, guanosine cyclic 2',3'-phosphate; EDTA, ethylenediaminetetraacetic acid; 2'-GMP, guanosine 2'-phosphate; GpC, guanylyl(3'-5')cytidine; GpU, guanylyl(3'-5')uridine; IPTG, isopropyl β-D-thiogalactopyranoside; MES, 2-(*N*-morpholino)ethanesulfonic acid; rms, root mean square; Tris, tris(hydroxymethyl)aminomethane; UpU, uridylyl(3'-5')-uridine.

0006-2960/90/0429-9064$02.50/0

(1988) for more refined data]. The folded structure consists of a single 4.5-turn α-helix which is packed over a 4-stranded antiparallel β-sheet.

RNase T_1 cleaves the P–O5′ ester bond specifically at the 3′ side of guanosine residues. The first step in the reaction consists of a transesterification and results in guanosine cyclic 2′,3′-phosphate. This cyclic phosphodiester may, in a second step, be hydrolyzed to yield 3′-guanylic acid. The chemical mechanism for transesterification involves a nucleophilic attack of the 2′-oxygen on the adjacent 3′-phosphate. The RNase T_1 catalyzed transesterification follows an in-line mechanism, implying a base and an acid located on either side of the scissile bond (Eckstein et al., 1972). The general base enhances the nucleophilicity of the 2′-oxygen and withdraws the 2′-hydroxyl proton during transesterification. The acid protonates the 5′-oxygen, thereby facilitating the expulsion of the leaving group.

On the basis of the active-site geometry, the stereochemistry of the reaction, and early biochemical data [see Takahashi and Moore (1982) and references cited therein], a mechanism has been put forward which includes the proposal that Glu58 acts as base catalyst along with His92, which protonates the O5′ of the adjacent ribose (Heinemann & Saenger, 1982). This hypothesis is supported by the observation that Glu58 and His92 are conserved in all enzymes belonging to the homologous family of microbial ribonucleases (Hill et al., 1983). Recently, Nishikawa et al. (1987) reported that the His40Ala and His92Ala RNase T_1 mutants are inactive while mutants in which Glu58 is replaced by Gln, Asp, or Ala retain considerable activity. On the basis of these observations, they proposed a new mechanism for the action of RNase T_1 in which His40 and His92 act as base and acid catalyst, respectively. Crystal structure data do not rule out that His40 and not Glu58 engages in catalysis as base catalyst; the distance of the 2′-oxygen to both the Glu58 carboxylate group and the His40 imidazole ring is very similar (Arni et al., 1988).

In the present paper, we describe the overproduction of the naturally occurring and some mutant RNase T_1 enzymes in *Escherichia coli*. For some key mutants, we report the kinetic parameters, the pH/rate profiles, and the NMR-determined pK_a values of the histidine residues. The results resolve the controversy concerning the functions of His40, Glu58, and His92 in catalysis of dinucleotide transesterification.

Experimental Procedures

Chemicals and Enzymes. Authentic (i.e., purified from *Aspergillus oryzae*) RNase T_1 was purchased from Bethesda Research Laboratories. The following T_1 ribonuclease substrates were used: the dinucleotides GpC and GpU, Sigma; RNA from Torula yeast (type VI), Sigma; bakers' yeast RNA, Cooper biomedical. Common reagents were purchased at the highest purity available. Other materials and their sources were as follows: Klenow fragment, Boehringer Mannheim; T4 DNA ligase and [α-^{35}S]dATP, Amersham; polynucleotide kinase, New England Biolabs; restriction endonucleases, (di)deoxynucleoside triphosphates, Q-Sepharose FF, and Sephacryl S-200 HR, Pharmacia; IPTG, Research Organics Inc.; D_2O, NaOD, and DCl, Aldrich.

Bacterial Strains, Media, and Plasmids. The su$^-$ strain WK6 [Δ(*lac-proAB*), *galE*, *strA*/F′*lacI*^{q}, *lacZ*ΔM15, *proA*$^+$*B*$^+$] and the DNA-mismatch repair-deficient strain WK6mutS [*mutS*::Tn10, otherwise isogenic to WK6] (Zell & Fritz, 1987) were used in the mutation construction experiments. WK6 also served as the host for expression of RNase T_1. Both strains were regularly streaked on minimal A plates (Miller, 1972) for selection of the F′*lacpro* episome. Bacteria were routinely grown at 37 °C in LB medium. TB medium, in which cells can be grown to high saturation density (Tartof & Hobbs, 1988), was used for the induced synthesis of RNase T_1 on a preparative scale. The plasmid pMT416 (Hartley, 1988) was used as a source of the P_{tac} promoter (De Boer et al., 1983) and the *phoA* secretion signal. The vectors pMa5-8 and pMc5-8 have been described by Stanssens et al. (1989).

Expression Vector Construction. All DNA manipulations were carried out by using standard procedures (Maniatis et al., 1982). The chemical synthesis of an RNase T_1 coding region has previously been described (Quaas et al., 1988). We used oligonucleotide-directed mutagenesis to engineer a *Pst*I site in front of the gene such that the sequence at the first codon (*GCT*; Ala) reads -CTGCA*GCT*-. Similarly, the expression signals (i.e., the P_{tac} promoter and a *phoA* region including the Shine–Dalgarno sequence and the secretion signal) were made accessible by introduction of a *Kpn*I site (-*GCG*GTACC-, *GCG* codes for the last amino acid residue of the *phoA* signal). Following digestion of the respective constructs with *Pst*I and *Kpn*I and treatment with DNA polymerase I (Klenow fragment), the *phoA* and RNase T_1 regions were fused by blunt-end ligation. The precise junction between the *phoA* signal and the RNase T_1 coding region, predicted by the construction scheme, was verified by DNA sequencing. The assembled P_{tac}-*phoA*-RNase T_1 expression cassette, contained on a 507 bp *Eco*RI–*Hin*dIII fragment, was inserted into the polylinker of both pMa5-8 and pMc5-8. The recombinant plasmids were designated pMa5-RT1 and pMc5-RT1.

Induced Synthesis and Purification of Recombinant RNase T_1. An overnight culture of WK6, containing either expression vector, was diluted 100-fold in TB medium. Expression of RNase T_1 was induced by the addition of IPTG (0.1 mM) when the culture had reached a density of $A_{650nm} \approx 1$. The cells were harvested by centrifugation after an induction period of 6–16 h. The periplasmic proteins were isolated from the cell pellet by an osmotic shock (Neu & Heppel, 1965). The periplasmic fraction was loaded onto a Q-Sepharose FF anion exchanger which was equilibrated with 50 mM phosphate buffer (pH 7.2). Proteins were eluted with a 50–500 mM phosphate gradient. The fractions containing RNase activity (visualized by means of an RNA–agar plate test, see below) were pooled and further purified by gel filtration through a Sephacryl S-200 HR column using 50 mM NH_4HCO_3 as the running buffer. Proteins were freeze-dried and stored at 4 °C. The yield was generally about 100 mg of pure RNase T_1 per liter of cell culture.

Protein Sequencing. N-Terminal sequence determination was performed on an Applied Biosystems 470A gas-phase sequenator.

Oligonucleotide-Directed Mutagenesis. The vectors pMa5-RT1 and pMc5-RT1 harbor the origin of replication of filamentous phage f1, thus allowing expression, oligonucleotide-directed mutagenesis, and sequencing of the RNase T_1 coding region to be carried out without any recloning step. The antibiotic resistance markers present on the pMa/pMc twin vector system allow a selection in favor of mutant progeny. Mutation construction experiments were performed as described (Stanssens et al., 1989). Oligonucleotides were synthesized by the phosphoramidite method (Beaucage & Caruthers, 1981) on an Applied Biosystems 380A DNA synthesizer and purified by polyacrylamide gel electrophoresis as described (Wu et al., 1984). Clones producing an RNase T_1 protein with a reduced ribonucleolytic activity and/or an

altered electrophoretic mobility on native polyacrylamide gel were retained (for more details on the screening, refer to Results). These putative mutant clones were infected with helper phage M13KO7 (Vieira & Messing, 1987) for production of single-stranded DNA, and the presence of the intended mutation was confirmed by sequencing (Sanger et al., 1977); two oligonucleotide primers were used to read the entire sequence of each mutant gene.

Enzyme Activity Assays and Kinetics. All experiments were performed at 35 °C. For wild-type as well as mutant forms of RNase T_1, protein concentrations were determined spectrophotometrically at 278 nm where $A_{0.1\%} = 1.9$ (Egami et al., 1964).

(*a*) *RNA–Agar Plate Assay.* The ribonucleolytic activity of bacterial lysates was measured in a semiquantitative way on agar plates supplemented with 0.5% yeast Torula RNA. The assay, based on the conversion of RNA to acid-soluble oligonucleotides, was carried out as described by Hartley and Smeaton (1973).

(*b*) *Specific Activity.* The specific activity, based on the rate of conversion of RNA to acid-soluble oligonucleotides, was determined as described (Egami et al., 1964). Reactions were performed in 0.2 M Tris-HCl (pH 7.5)/0.02 M EDTA using 1.2% bakers' yeast RNA as substrate.

(*c*) *Kinetics of GpC Transesterification.* Steady-state kinetic parameters, K_m and k_{cat}, for the transesterification of GpC were determined from initial velocities by measuring the absorbance increase at 280 nm (Zabinski & Walz, 1976). Assays were performed in 100 mM MES, 100 mM NaCl, and 2.5 mM EDTA at pH 6.0 (ionic strength 0.15 M). The GpC concentration (determined by taking ϵ_{280nm} as 1.26×10^4 M^{-1} cm^{-1}; Zabinski & Walz, 1976) was varied between 0.0192 and 1.44 mM. Reactions were started by adding 0.53, 1538, 430, 17.2, 38.4, and 879 nM of wild-type, His40Ala, His40Lys, Glu58Ala, Glu58Gln, and His92Gln RNase T_1, respectively. At high substrate concentrations, 0.1- and 0.5-cm path-length cuvettes were used to circumvent the high background absorbance of the substrate. Kinetic parameters were obtained by nonlinear regression.

(*d*) *pH Dependence of* k_{cat}/K_m. The pH dependence was determined for the dinucleotide substrate GpC in the pH range 2.8–9. The buffers had an ionic strength of 0.1 M and were sodium formate/formic acid at pH 2.8–4.0, sodium acetate/acetic acid at pH 3.8–6.0, imidazole hydrochloride/NaOH at pH 6.0–7.8, and Tris-HCl/NaOH at pH 7.8–9.0. GpC was added to the buffer at a final concentration of 10 μM. Reactions were started by adding enzyme and followed by measuring the absorbance increase at 280 nm. For wild-type RNase T_1, the chosen substrate concentration (10 μM) is at least 10 times lower than the K_m value in the pH range studied (Osterman & Walz, 1978). We confirmed that this condition is also met for the His40Lys and Glu58Ala enzymes (data not shown). At substrate concentrations much lower than K_m, the GpC transesterification reaction follows first-order kinetics with rate constant V_{max}/K_m; this constant can be derived from a single progress curve recording (Fersht & Renard, 1974). The procedure allows the collection of many data and eliminates the need to consider the pH dependence of the difference molar extinction coefficient. Experimental progress curves were analyzed by nonlinear regression and the obtained pH dependence profiles fitted to theoretical curves by use of the program package ENZFITTER (Leatherbarrow, 1987).

(*e*) *pH Dependence of* k_{cat}. The pH dependence of k_{cat} was determined for the Glu58Ala RNase T_1 catalyzed transesterification of the dinucleotide GpU. Initial velocities were measured at saturating substrate concentrations by following the absorbance increase at 280 nm in a 0.1-cm path-length cuvette. The reactions were followed in the pH range 3.5–9; the 0.1 M standard buffers were the same as described above. The GpU concentration was determined by taking ϵ_{280nm} as 1.06×10^4 M^{-1} cm^{-1}. The experimental data were corrected for the pH dependence of the difference molar extinction coefficient (Zabinski & Walz, 1976). The data were analyzed with the program ENZFITTER (Leatherbarrow, 1987).

^1H NMR Measurements. Five milligrams of protein was dissolved in D_2O containing 100 mM NaCl and kept at pH 8.5 and 35 °C for 1 h to remove exchangeable NH protons. Spectra were taken in the pH range 5–10 at intervals of 0.2 units. The pH, adjusted with DCl or NaOD, was measured in the NMR sample tube using a 4-mm outer diameter electrode (Ingold). The pH meter was calibrated against standard H_2O buffers. Readings were not corrected for possible isotope effects. Spectra were recorded at 35 °C on a 600-MHz Varian VXR-S spectrometer using presaturation of the HOD solvent resonance. Plots of the chemical shift vs pH were fitted with the following function: $(SK_a + S^+H)/(K_a + H)$ where K_a is the acid dissociation constant, H is the proton concentration, and S and S^+ are the proton chemical shifts of the fully deprotonated and protonated histidine, respectively.

Crystal Structure Analysis. The atomic coordinates of the RNase T_1–2′-GMP complex were taken from the Protein Data Bank (Bernstein et al., 1977). Coordinates of barnase [determined by Mauguen et al. (1982)] were kindly provided by Dr. S. Wodak. The structures of this pair of ribonucleases were superimposed by matching the α-carbon positions of structurally well-conserved stretches of polypeptide. These segments, essentially corresponding to the β-sheet's, were taken from Hill et al. (1983) and are the following: 38–48, 54–62, 74–86, 88–90, 91–92, and 100–102 for RNase T_1; 52–62, 69–77, 84–96, 97–99, 101–102, and 103–105 for barnase. The best overlap between these corresponding fragments was found by least-squares fitting (rms distance = 1.28 Å) using the BRUGEL software package (Delhaise et al., 1984). Fitted structures were displayed on an Evans & Sutherland PS390 graphic terminal.

RESULTS

Overproduction, Purification, and Characterization of Recombinant RNase T_1. A gene that codes for RNase T_1 fused at its N-terminal end to the *E. coli phoA* secretion signal peptide was constructed. The expression vector contains this chimeric gene under the transcriptional control of the P_{tac} promoter (see Experimental Procedures). WK6 (*lacI^q*) cells harboring this expression vector were found to direct the efficient production of RNase T_1 upon derepression of the promoter with IPTG. Overproduction of RNase T_1 is readily visualized by fractionation of cellular extracts on a native polyacrylamide gel (Figure 1A); RNase T_1, a small and acidic protein, has a high mobility on this type of gel and is therefore well separated from the bulk of host proteins. Concurrent with the appearance of the characteristic protein band on the native gel, a dramatic increase in ribonucleolytic activity was observed (Figures 1B and 2). The enzymatic activity measurements show that induction results in at least a 50-fold increase in the expression level and that the RNase T_1 protein amounts to about 20 mg/L per A_{650nm} unit. Virtually all of the enzymatic activity could be released with an osmotic shock, demonstrating that active RNase T_1 accumulates in the periplasmic space. This is in accordance with the observation that the bacterial host is only slightly impaired in its growth rate in the presence

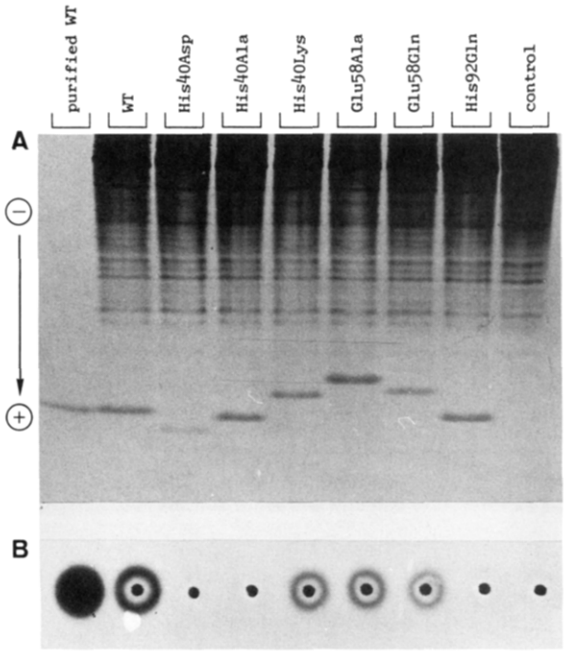

FIGURE 1: Analysis of protein samples (A) on a native gel and (B) by means of an RNA plate test. Wild-type (WT) and mutant clones (the mutation is indicated above the lanes) were induced for 4 h; cellular extracts were prepared by sonication. The gel (15% polyacrylamide/Tris-HCl, pH 8.8) was prepared essentially according to Davis (1964). The first lane contains 8 μg of purified RNase T_1. Other lanes contain the equivalent of 5×10^8 cells. The control shows the protein pattern of an uninduced culture. RNA plate test: the ribonucleolytic activity of the protein samples is seen as a clearance zone (dark halo) in the RNA precipitate that forms upon addition of 1 M sulfuric acid. In the case of the crude lysates, a protein precipitate forms immediately around the wells.

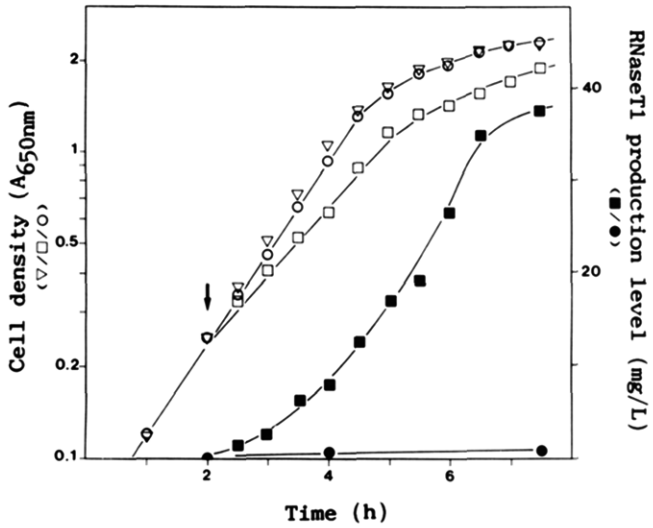

FIGURE 2: Induced synthesis of RNase T_1 and its effect on the growth rate of host cells. The time of induction is indicated by an arrow. Right ordinate: the amount of RNase T_1, produced by uninduced (●) and induced (■) WK6[pMc5-RT1], was determined by comparing the ribonucleolytic activity of cellular extracts against that of known quantities of authentic RNase T_1. Extracts were prepared by sonication. The activity was measured by following $\Delta A_{298.5nm}$ (Oshima et al., 1976) on hydrolysis of yeast Torula RNA. Left ordinate: the growth curves of uninduced (○) and induced (□) WK6[pMc5-RT1] are compared with the growth rate of strains WK6 harboring a control plasmid that does not contain the RNase T_1 expression cassette (▽, no curve was drawn through the data points).

of IPTG when the degradative RNase T_1 enzyme is maximally expressed (Figure 2). Recently, Quaas et al. (1988) have shown that the signal peptide of the OmpA protein may also be used for the production of RNase T_1 as a secretory protein.

Table I: Activities of Wild-Type and Mutant RNase T_1 Enzymes

RNase T_1	RNA[a] (%)	GpC[b] K_m (μM)	GpC[b] k_{cat} (min^{-1})	GpC[b] k_{cat}/K_m (min^{-1} mM^{-1})
wild type	100	134	18600	141060
Glu58 to Ala	10.4	85	660	7740
Glu58 to Gln	6.2	296	321	1086
His40 to Lys	3.1	426	260	612
His40 to Ala	<0.1	292	9.8	33.5
His40 to Asp	<0.1		ND[c]	
His92 to Gln	<0.1	201	14.6	69.8

[a] The relative activities for RNA hydrolysis were determined as described under Experimental Procedures. The specific activity of wild type was 386000 units/mg. [b] The kinetics of transesterification of GpC were measured at 35 °C, pH 6.0, in a 0.15 M ionic strength buffer. [c] ND, not determined.

The RNase T_1 sequestered in the periplasmic space was released by an osmotic shock and further purified by two chromatographic steps as described under Experimental Procedures.

N-Terminal protein sequencing of the purified recombinant enzyme revealed a uniqe amino-terminal sequence, identical with that of *Aspergillus oryzea* RNase T_1. Thus, the PhoA–RNase T_1 precursor undergoes correct processing. The recombinant and the *A. oryzae* RNase T_1 were found to have the same specific activity and to yield the same cleavage products upon partial digestion of 5′-end-labeled yeast 5S RNA (data not shown). Urea denaturation as well as thermal unfolding experiments show that the conformational stabilities of overproduced and authentic RNase T_1 are identical (Shirley et al., 1989). The above data demonstrate that the RNase T_1 overproduced in *E. coli* is both functionally and physically indistinguishable from the authentic protein.

Generation of RNase T_1 Mutants by Oligonucleotide-Directed Mutagenesis. Mutation construction experiments were carried out as described under Experimental Procedures. The following single amino acid substitutions were engineered: His40Asp, His40Ala, His40Lys, Glu58Ala, Glu58Gln, and His92Gln. Note that two isoforms of RNase T_1 exist: one with Gln, the other with Lys at position 25. The wild-type and mutant enzymes discussed in this paper all contain a Lys residue at position 25.

The fact that mutagenesis and expression are carried out from the same vector enabled us to screen for the desired mutants at the protein level. The following two approaches were used: (a) measurement of the ribonucleolytic activity of cellular extracts of induced cultures on RNA–agar plates (see Experimental Procedures), whereby clones producing a mutant enzyme with a substantially decreased catalytic activity can be discriminated from those producing wild-type enzyme, and (b) analysis of the same extracts on a native polyacrylamide gel, revealing the presence of a mutation which, under the electrophoretic conditions, alters the net charge of the protein. Figure 1 demonstrates that each desired mutant could be identified by at least one of the above approaches. Final confirmation of the presence of the intended mutation was obtained by DNA sequence analysis.

The synthesis of mutant proteins was induced as described for wild-type RNase T_1. All mutants were expressed at a level comparable to wild-type enzyme (Figure 1A) and were found to behave as wild type in the purification scheme.

Steady-State Kinetics. (a) RNA Hydrolysis. Specific activities, based on the rate of conversion of yeast RNA to acid-soluble oligonucleotides, were determined for all mutants. Table I compares the specific activities of the mutant enzymes with that of wild-type RNase T_1. The His40Lys, Glu58Ala,

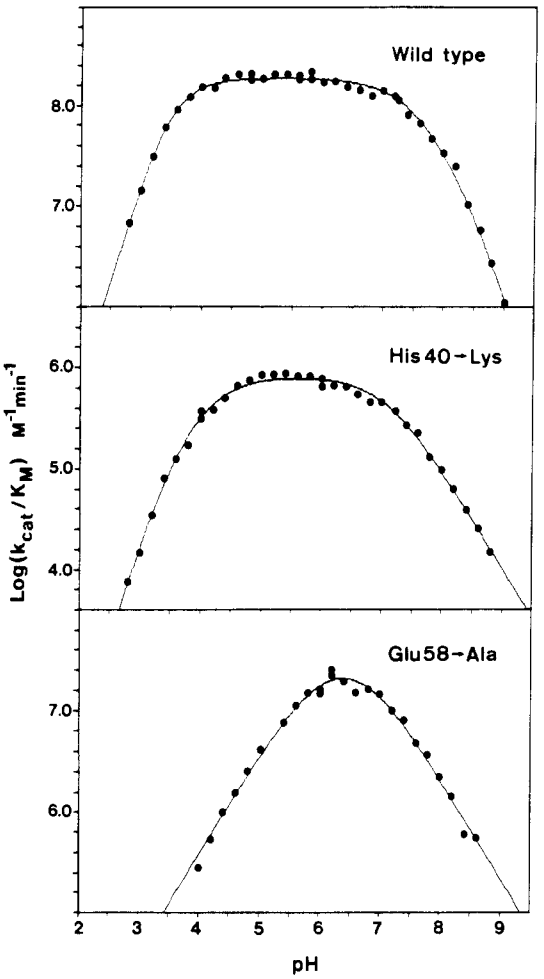

FIGURE 3: Plots of log (k_{cat}/K_m) versus pH for GpC transesterification by wild-type, His40Lys, and Glu58Ala RNAse T_1. All experiments were conducted at 35 °C in 0.1 M standard buffers; other details are under Experimental Procedures. For wild-type enzyme, the curve giving best fit to the experimental data was generated with the use of the equation given in the text. For the mutants, some of the molecular parameters according to Figure 4 were given limit values: $K_D = 0$ for His40Lys; $K_D = 0$ and $K_A = \infty$ for Glu58Ala. Best-fit parameters are shown in Table II.

and Glu58Gln RNase T_1 enzymes possess considerable residual activity toward RNA. In contrast, no activity could be detected in the case of the His40Ala, the His40Asp, or the His92Gln substitution. The relative activities found for the various enzymes are in good agreement with the RNA plate analysis presented in Figure 1B.

(b) GpC Transesterification. The conversion of GpC to cGMP and cytosine can be easily followed spectrophotometrically at 280 nm (Osterman & Walz, 1978). Table I lists the steady-state kinetic parameters for this reaction for wild-type, His40Ala, His40Lys, Glu58Ala, Glu58Gln, and His92Gln RNase T_1. All amino acid substitutions result in small changes in K_m. Consistent with the observations made by Nishikawa et al. (1987), we find that the catalytic activity is not severely compromised by Glu58 mutations. The His40Ala and His92Gln mutations reduce k_{cat} by about 3 orders of magnitude. Installation of a lysine at position 40 partially compensates for the removal of the naturally occurring side chain.

(c) pH Dependence of k_{cat}/K_m for GpC Transesterification. The pH dependence of k_{cat}/K_m generally follows the ionization of acid–base groups on the free enzyme and the free substrate that are involved in binding and/or catalysis. pH dependence studies performed by Osterman and Walz (1978) on authentic

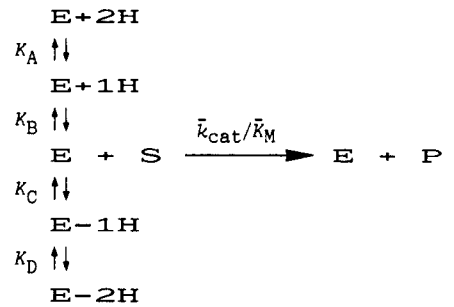

FIGURE 4: Reaction scheme proposed to explain the pH dependence of GpC transesterification by wild-type RNase T_1. S, substrate; P, product; E, free enzyme; $\pm n$H, nth relevant protonation/deprotonation stage. $\bar{k}_{cat}/\bar{K}_m$ is the pH-independent apparent second-order rate constant. K_A, K_B, K_C, and K_D are macroscopic acid dissociation constants. The pH profile of the His40Lys mutant enzyme is consistent with this model, if the second deprotonation stage (E–2H) is ignored ($K_D = 0$). The observations made for the Glu58Ala mutant can be explained by taking only a single protonation/deprotonation stage into consideration ($K_D = 0$ and $K_A = \infty$).

enzyme suggested the requirement of two deprotonated and two protonated groups. On the basis of the pK values revealed by the pH dependence, combined with information from independent studies, it was concluded that the deprotonated groups correspond to Glu58 and an as yet unidentified carboxyl group. The protonated groups were tentatively identified as His40 and His92. We reinvestigated the pH profile of k_{cat}/K_m for GpC transesterification using recombinant RNase T_1 and compared it to the profiles we obtained for His40Lys and Glu58Ala RNase T_1. Plots of log (k_{cat}/K_m) versus pH are shown in Figure 3. Our data on wild type-enzyme are consistent with those obtained by Osterman and Walz (1978); the absolute values of both the ascending and descending slopes of log (k_{cat}/K_m) versus pH are significantly greater than 1, suggesting the necessity of two proton-dissociated groups (hereafter called bases) and two proton-associated groups (hereafter called acids) for optimal activity. A formal mechanism that meets the observed pH dependence was proposed by Osterman and Walz (1978) and is presented in Figure 4. The following equation relates the experimental data to the molecular parameters according to Figure 4:

$$k_{cat}/K_m = \frac{\bar{k}_{cat}/\bar{K}_m}{1 + H^2/K_AK_B + H/K_B + K_C/H + K_CK_D/H^2}$$

where $\bar{k}_{cat}/\bar{K}_m$ is the ratio of the pH-independent values of the turnover number and the Michaelis constant, where K_A, K_B, K_C, and K_D are macroscopic acid dissociation constants, and where H represents the proton concentration. The experimental data for the wild-type enzyme were fitted to this theoretical function by nonlinear regression (see Figure 3). Best-fit parameters are listed in Table II.

Important differences exist between the pH dependence of the mutants and that of wild-type enzyme. The pH profile of the His40Lys RNase T_1 is characterized by an ascending slope of 1.6 and a descending slope of −0.95, suggesting the involvement of two bases and, in contrast to wild type, only a single acid. The observed pH dependence may be interpreted in terms of the mechanism given in Figure 4 in which the second stage of deprotonation is ignored. The fitted pH dependence curve for this mutant, shown in Figure 3, was generated by the above equation in which K_D equals zero. The slopes characterizing Glu58Ala RNase T_1 (1.1 and −1) indicate that the substrate binding and catalytic potential depend on a single base and a single acid. The experimental data for Glu58Ala were therefore fitted to a simple bell-shaped curve

Table II: Best-Fit Parameters for the pH Dependence of k_{cat}/K_m for GpC Transesterification: Comparison with the Histidine pK_a's Derived from NMR

	wild type	His40Lys	Glu58Ala
	Kinetics[a]		
ascending slope	1.6	1.6	1.1
descending slope	−1.65	−0.95	−1.0
k_{cat}/K_m (min^{-1} μM^{-1})	188.3	0.83	37.9
pK_A	3.2	3.5	
pK_B	3.8	4.1	6.0 (6.3)
pK_C	7.4 (7.2)	7.1	6.8 (7.0)
pK_D	8.5 (7.9)		
	NMR[b]		
pK_a^{His27}	7.1	7.1	7.2
pK_a^{His40}	7.7		6.5
pK_a^{His92}	7.4	ND	6.8

[a] See text for details of the analysis. The pK values (estimated standard errors <0.2) are macroscopic constants which refer to stages of ionization of the protein (see Figure 4) and are not the true microscopic constants of particular side chains. [b] Microscopic acid dissociation constants. NMR measurements were performed at 35 °C and 0.1 M ionic strength so that the data can be compared with kinetics. The experimental data (standard error <0.1) have not been corrected for possible deuterium isotope effects. ND, this value could not be determined (see text). Macroscopic constants, calculated from the NMR-determined His40 and His92 pK_a's, are given in parentheses next to the kinetically determined pK's which we assume reflect His40 and His92 titrations. The calculated values equal −log ($K_a^{His40} + K_a^{His92}$) and −log [$1/K_a^{His40} + 1/K_a^{His92}$)].

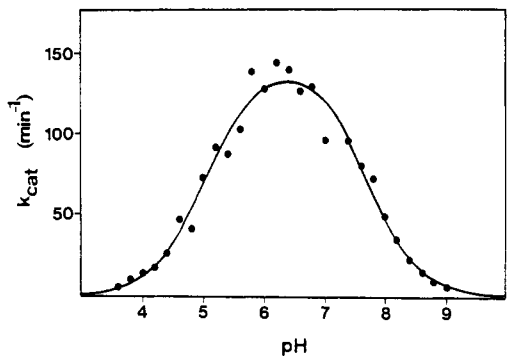

FIGURE 5: Plot of k_{cat} versus pH for GpU transesterification by Glu58Ala RNase T_1. All experiments were conducted at 35 °C in 0.1 M standard buffers; other details are under Experimental Procedures. The bell-shaped curve giving best fit to the data is shown.

($K_D = 0$ and $K_A = \infty$). Fitted parameters for both mutants are listed in Table II.

(d) pH Dependence of k_{cat} for GpU Transesterification by Glu58Ala RNase T_1. The pH dependence of k_{cat} generally follows the critical ionization of the enzyme–substrate complex whose decomposition is rate limiting. The pH dependence of k_{cat} for the transesterification of GpU by wild-type enzyme (0.2 M ionic strength; 25 °C) revealed the involvement of one base and one acid with apparent pK's of 3.0 and 8.3, respectively (Osterman & Walz, 1978). We investigated the pH profile of k_{cat} for Glu58Ala RNase T_1 using the same substrate (see Figure 5). The experimental data form a bell-shaped pH curve generated by two groups with macroscopic pK's estimated at 5.1 and 7.7.

Determination of Histidine Ionization Constants by NMR. The resonances of most RNase T_1 protons have been assigned by two-dimensional ^1H NMR spectroscopy (Hoffmann & Rüterjans, 1988). We measured the pH dependence of the chemical shifts of the C2 and C4 histidine protons of wild-type, His40Lys, and Glu58Ala RNase T_1. Only the proton resonances which could be unambiguously followed over the entire pH range (5–10) were used for pK_a determination. Wild-type, His40Lys, and Glu58Ala RNase T_1 show similar titration curves for the His27 C4–H resonance. For all three enzymes, the proton peak shifts from 6.7 to 6.2 ppm when the pH is raised from 5 to 10; the inflection points are almost identical (see Table II). The C2–H signal of His40 lies at the other end of the aromatic region and was followed in order to measure the pK_a of this residue in wild-type and Glu58Ala RNase T_1. The His40 C2–H peak moves between 8.4 and 7.6 ppm over the pH interval. The deduced pK_a's are 7.7 and 6.5 for wild-type and Glu58Ala enzyme, respectively. For wild-type enzyme, the C2–H (7.6–7.0 ppm) and C4–H (7.1–6.6 ppm) resonances of His92 were followed: both signals titrate with a pK_a of pH 7.4. The His92 C4–H resonance of Glu58Ala RNase T_1 shifts from 7.0 to 6.6 ppm and titrates with a pK_a of 6.8. For His40Lys RNase T_1, we were unable to determine the pK_a of His92. The C2–H and C4–H proton peaks of His92 could only be followed between pH 5 and 7. Above pH 7, the signals broaden and disappear from the spectrum. This is probably due to intermediate chemical exchange.

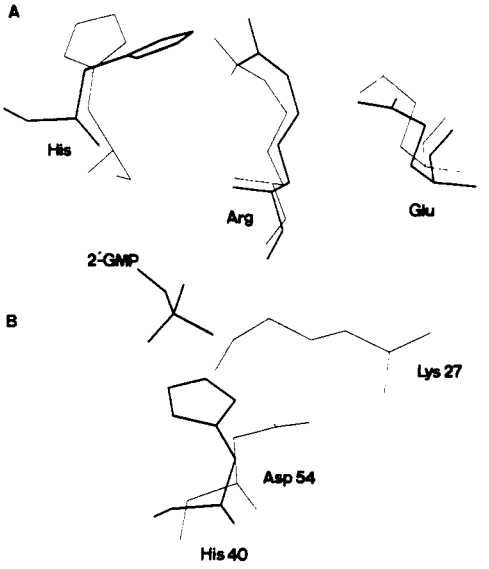

FIGURE 6: View of sections of the superimposed structures of RNase T_1 (bold lines) and barnase (thin lines). (A) Overlap between RNase T_1 active-site residues (Glu58; Arg77; His92) and the homologous residues of barnase (Glu73; Arg87; His102). (B) His40 of RNase T_1: structural relationship to Lys27 and Asp54 of barnase. The phosphate moiety of the RNase T_1 inhibitor 2′-GMP is also shown. For details, refer to the text.

His40 of RNase T_1: Relationship to Asp54 and Lys27 of Barnase. The microbial ribonucleases can be divided in two major classes: (1) the T_1 group, containing the fungal ribonucleases; (2) the bacterial enzymes of which barnase is a representative (Hill et al., 1983). Sequence alignments and structural comparisons of several of these ribonucleases have shown that His40 of RNase T_1 is conserved in all fungal ribonucleases, but is not found in any of the bacterial enzymes; the equivalent in barnase is the residue Asp54 (Hill et al., 1983). This is a notable difference in view of our data which show that His40 is implicated in catalysis; more specifically, we find that replacement of His40 by an Asp residue drastically reduces the rate of RNA hydrolysis (Table I). We therefore decided to reinvestigate the positions of His40 and Asp54 in their respective active sites. To this end, the 3D structures of RNase T_1 and barnase were fitted on each other as described under Experimental Procedures. Figure 6A shows that the α-carbons as well as the side chains of the strictly conserved active-site residues Glu58, Arg77, and His92 of RNase T_1 match quite well with their equivalents in barnase

(e.g., Glu73, Arg87, and His102). Figure 6B compares the position of His40 of RNase T_1 with those of Lys27 and Asp54 of barnase. It can be seen that the side chains of His40 and Asp54 point in opposite directions while their Cα atoms were put within only 0.5 Å of each other by the least-squares fit. The Asp54 side chain is oriented away from the catalytic site. Instead, the Lys27 side chain of barnase is directed toward the phosphate moiety of the 2′-GMP molecule (T_1 inhibitor), and the ϵ-amino group approaches the His40 imidazole ring (the distances of the Nϵ and the Nδ of the imidazole are 0.42 and 2.48 Å, respectively). The congruency of these groups (their separation is probably within side chain movement distance) suggests that barnase–Lys27 is the functional analogue of T_1–His40.

Discussion

T_1 ribonuclease has been produced in *E. coli*. The enzyme is directed to the periplasm and can be easily purified in large quantities. The recombinant protein is identical with the authentic enzyme from *Aspergillus oryzea* in every physical and catalytic parameter tested so far. Overproduction in *E. coli* renders RNase T_1 amenable to further detailed structure–function analyses.

The active-site residues, His40, Glu58, and His92, have been implicated in catalysis and/or binding by protein chemical, spectroscopic, and X-ray studies. Their specific roles in the catalytic mechanism are, however, still a subject of discussion. We replaced them by site-directed mutagenesis and analyzed the kinetic consequences. For the conversion of GpC to cGMP and cytosine, all investigated amino acid replacements result in a substantial decrease in k_{cat}, concomitant with only small changes in the Michaelis constant (Table I); this indicates that His40, Glu58, and His92 are involved in catalysis rather than in substrate binding.

A clue as to what functions His40, Glu58, and His92 fulfill is given by the pH profiles of k_{cat}/K_m for GpC transesterification by wild-type enzyme and some selected mutants. Full enzymatic activity of recombinant wild-type enzyme was found to depend on two groups that must be deprotonated (bases) and two groups that must be protonated (acids). This is in agreement with the original observations made by Osterman and Walz (1978) using authentic RNase T_1. These authors suggested that Glu58 and an unidentified carboxyl group correspond to the bases and that His40 and His92 represent the acids. The assignment of the acids was essentially based on the observation that the macroscopic constants associated with the first and second stage of deprotonation (K_C and K_D in Figure 4) agree well with the microscopic dissociation constants of His40 and His92 determined by NMR. Our kinetic and NMR data reaffirm this argument. The microscopic constants of His40 and His92 are too close to identify them with particular macroscopic pK's. Corresponding macroscopic parameters may, however, be calculated from the microscopic ones (see Table II) if one assumes that the two ionizing groups have no influence on one another (Dixon & Webb, 1979). Given the experimental errors, possible shortcomings of the theoretical formalism (Knowles, 1976), and the assumption that the pK_a's measured in D_2O equal those in water, the calculated and measured macroscopic constants agree quite well. That the activity of wild-type enzyme depends on the protonated form of His40 is strongly supported by the pH profile characterizing the His40Lys mutant. This mutation results in loss of one ionization at the alkaline side [i.e., the descending slope of log (k_{cat}/K_m) vs pH changes from 1.6 to 1.0], consistent with the replacement of one of the acids (His40) by a residue (Lys) which is protonated over the entire pH range studied. Taken together, the data demonstrate that optimal activity of wild-type enzyme depends on the protonated form of His40. This residue can, therefore, not act as base catalyst, contradictory to the conclusion reached by Nishikawa et al. (1987). Replacement of His40 by a lysine has, apart from the lowered value of $\bar{k}_{cat}/\bar{K}_m$ and from the loss of one ionization, little effect on the remaining parameters of the pH profile. This observation suggests that the activities of wild-type and His40Lys RNase T_1 both depend on the deprotonated form of Glu58, on an unidentified carboxylate ion, and on the protonated form of His92. The pH profiles of the wild-type and His40Lys enzymes are entirely consistent with the widely accepted view that Glu58 and His92 serve as base and acid catalyst, respectively (Heinemann & Saenger, 1982).

The high residual activities of Glu58Ala and Glu58Gln RNase T_1 (Table I) reaffirm the data previously reported by Nishikawa et al. (1987). This observation appears to contradict the assignmment of Glu58 as base catalyst. In barnase, replacement of the active-site general base Glu73 by an alanine was found to abolish all observable activity (<0.01%; Mossakowska et al., 1989). The analysis of the pH profile of Glu58Ala RNase T_1 resolves this apparent paradox. Consistent with the proposal that the protonation state of Glu58 is critical to the activity of wild-type enzyme, we observe that replacement with alanine has a marked effect on the pH dependence curve. The pH dependence of k_{cat}/K_m for the mutant enzyme fits to a bell-shaped curve generated by a single base and a single acid (see Results). The free enzyme pK's, estimated at 6.0 and 6.8, suggest that the imidazole side chains of histidine residues are involved. His40 and His92 are the evident candidates. The NMR data strengthen this notion. The Glu58Ala mutation has a significant effect on the pK_a's of both His40 and His92. They are reduced by 1.2 and 0.5 unit, respectively. The pronounced effect on His40 is in agreement with the proposal that this residue is in direct contact with Glu58 in free enzyme (Arata et al., 1979). Apparently, the carboxylate ion also stabilizes the protonated form of His92. The microscopic pK_a's of His40 and His92 predict a slightly higher pH optimum (6.65) than experimentally observed for the Glu58Ala enzyme (6.4), yet the macroscopic parameters revealed by kinetics agree well with those calculated from the pK_a's of both histidines (see Table II). Taking the results together, we conclude that the pH dependence of Glu58Ala RNase T_1 reflects the titrations of His40 and His92. (The pK_a of the unidentified carboxyl group, whose titration is reflected in the pH dependence of wild-type enzyme, is probably too low to be seen in the pH range studied for this mutant.) The pH dependence of k_{cat}/K_m could theoretically yield the pH dependence of the substrate binding reaction only. The bell-shaped pH profile of k_{cat} for the Glu58Ala mutant (macroscopic pK's estimated at 5.1 and 7.7) suggests that His40 and His92 are catalytically involved. Thus, whereas protonation of both histidines is essential for maximal activity of wild-type enzyme, one histidine is required in the deprotonated form for catalysis by Glu58Ala RNase T_1. We propose that this mutant is mechanistically similar to RNase A in that two histidine residues act as base and acid catalysts. The pH/rate profiles and the NMR data of the Glu58Ala mutant do not allow us to decide which of the two histidines is required in the deprotonated state for enzymatic activity. We believe that the role of base catalyst of Glu58Ala RNase T_1 must be attributed to His40. The His40 imidazole and the Glu58 carboxylate ion are located at comparable distances to the 2′-oxygen in the RNase T_1–2′-GMP complex and are

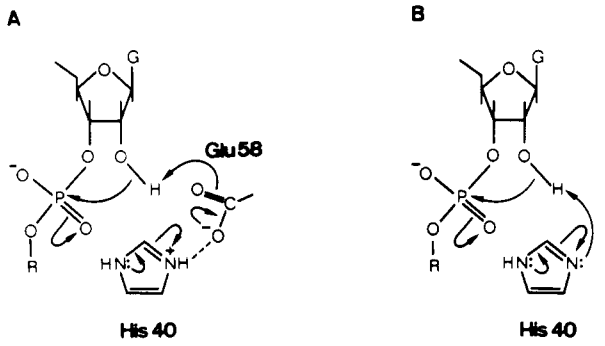

FIGURE 7: Tentative proposal for the role of His40 and Glu58 in transition-state formation. (A) Wild-type enzyme. The dashed line represents the interaction between His40 and Glu58. (B) Glu58Ala RNase T_1. See text for details.

situated at the same side of the phosphate group, opposite His92. Participation of His40 in acid base catalysis along with His92 seems therefore not to be in contradiction with the in-line mechanism proposed for the wild-type enzyme. Our data do not allow us to decide whether His40 directly accepts the proton from the 2′-OH or if it acts via a H_2O molecule which may occupy the cavity generated by substitution of an Ala residue for Glu58. The hypothesis that a distinct residue (His40) engages in catalysis as base when the true catalytic base (Glu58) is eliminated provides a satisfactory explanation for the remarkable observation that the Glu58Ala mutation does not reduce catalytic activity dramatically.

Our kinetic studies demonstrate that the protonated His40 side chain accounts for a factor of ~2000 in the overall rate acceleration of GpC transesterification by wild-type RNase T_1 (Table I). The charged His40 side chain may shield the negative charge of the phosphate anion prior to the nucleophilic attack of the 2′-oxygen. This kind of electrostatic catalysis has been found to be essential for the transesterification of UpU by imidazole or by imidazole/Zn^{2+} buffers (Anslyn & Breslow, 1989; Breslow et al., 1989). Alternatively, the positively charged residue may stabilize the second negative charge that develops during the formation of the pentacovalent transition-state complex. It may also stabilize the position and optimize the pK_a of Glu58 (Arni et al., 1988). Our preferred model for the mode of action of His40 is shown in Figure 7A. As suggested by previous studies (Arata et al., 1979; Heinemann & Saenger, 1982), we consider an interaction between Glu58 and His40 in the ground-state configuration of the enzyme–substrate complex. We suggest that this interaction couples the activation of the O2′ nucleophile by Glu58 to electrostatic stabilization of the transition state by the displaced charge of His40. In such a model, the imidazole cation would shield the negative charge which develops on one of the equatorial phosphate oxygens upon nucleophilic attack of the 2′-oxygen. This model is attractive in that it can be extrapolated to the Glu58Ala enzyme; in this mutant, His40 cannot shield the charge of the phosphate anion prior to the nucleophilic attack, but it may combine base catalysis with electrostatic stabilization of the second charge that develops during transition-state formation (Figure 7B). If shielding of the charge of the phosphate anion prior to the nucleophilic attack is an important aspect in catalysis by RNase T_1, we feel that a residue other than His40 must fulfill this role. Arg77, a conserved residue in all microbial RNases, is an excellent candidate.

Considering the critical role of His40 in RNase T_1 catalysis, it is quite remarkable that this residue is not conserved in the bacterial RNases of which barnase is the best known representative. Superposition of the RNase T_1 and barnase crystal structures indicates that the Lys27 side chain of barnase and the His40 imidazole of RNase T_1 occupy a similar position in the respective active sites (see Results and Figure 6). Mossakowska et al. (1989) recently demonstrated that replacement of Lys27 of barnase by Ala lowers the k_{cat} for dinucleotide transesterification by a factor of ~4000, similar to our observation for His40Ala RNase T_1. In total, these observations suggest that His40 of RNase T_1 and Lys27 of barnase are functional analogues, having a positive charge in common that contributes to electrostatic catalysis. It is interesting to note that the two residues superimpose only at the side chain level. At the backbone level, His40 of RNase T_1 fits to Asp53 of barnase (Hill et al., 1983; and Figure 6B). This structural analysis is further supported by the observation that His40Asp RNase T_1 is inactive (Table I) whereas Asp53Ala barnase retains considerable activity (Mossakowska et al., 1989). Thus, it would appear that His40, although strictly conserved only in the fungal RNases, has a functional counterpart in the bacterial enzymes.

ACKNOWLEDGMENTS

We thank C. Opsomer for expert technical assistance and Drs. C. Thoen and Y. McKeown for help at an early stage of this research. We are indebted to Dr. R. Hartley for providing us with pMT416. Thanks are due to Drs. A. Lambeir, M. Lauwereys, and S. Wodak for helpful discussions and suggestions. We thank Dr. M. De Maeyer for help with the BRUGEL package, J. Van Damme for protein sequence analysis, and A. Lenaerts for synthesis of oligonucleotides.

Registry No. L-His, 71-00-1; L-Glu, 56-86-0; L-Ala, 56-41-7; L-Gln, 56-85-9; L-Lys, 56-87-1; L-Asp, 56-84-8; GpC, 4785-04-0; RNase T_1, 9026-12-4.

REFERENCES

Anslyn, E., & Breslow, R. (1989) *J. Am. Chem. Soc. 111*, 4473–4482.

Arata, Y., Kimura, S., Matsuo, H., & Narita, K. (1979) *Biochemistry 18*, 18–24.

Arni, R., Heinemann, U., Tokuoka, R., & Saenger, W. (1988) *J. Biol. Chem. 263*, 15358–15368.

Beaucage, S. L., & Caruthers, M. H. (1981) *Tetrahedron Lett. 22*, 1859–1862.

Bernstein, F. C., Koetzle, T. F., Williams, G. J. B., Meyer, E. F., Jr., Brice, M. D., Rodgers, J. R., Kennard, O., Shimanouchi, T., & Tasumi, M. (1977) *J. Mol. Biol. 112*, 535–542.

Breslow, R., Huang, D.-L., & Anslyn, E. (1989) *Proc. Natl. Acad. Sci. U.S.A. 86*, 1746–1750.

Davis, B. J. (1964) *Ann. N.Y. Acad. Sci. 121*, 404–427.

De Boer, H. A., Comstock, L. J., & Vasser, M. (1983) *Proc. Natl. Acad. Sci. U.S.A. 80*, 21–25.

Delhaise, P., Bardiaux, M., & Wodak, S. J. (1984) *J. Mol. Graphics 2*, 103–106.

Dixon, M., & Webb, E. (1979) *Enzymes*, 3rd ed., Longman, London.

Eckstein, F., Schulz, H., Rüterjans, H., Haar, W., & Maurer, W. (1972) *Biochemistry 11*, 3507–3512.

Egami, F., Takahashi, K., & Uchida, T. (1964) *Prog. Nucleic Acid Res. Mol. Biol. 3*, 59–101.

Fersht, A. R., & Renard, M. (1974) *Biochemistry 13*, 1416–1426.

Hartley, R. W. (1988) *J. Mol. Biol. 202*, 913–915.

Hartley, R. W., & Smeaton, J. R. (1973) *J. Biol. Chem. 248*, 5624–5626.

Heinemann, U., & Saenger, W. (1982) *Nature (London) 299*, 27–31.

Hill, C., Dodson, G., Heinemann, U., Saenger, W., Mitsui, Y., Nakamura, K., Borisov, S., Tischenko, G., Polyakov, K., & Pavlovsky, S. (1983) *Trends Biochem. Sci. 8*, 364-369.
Hoffmann, E., & Rüterjans, H. (1988) *Eur. J. Biochem. 177*, 539-560.
Knowles, J. R. (1976) *CRC Crit. Rev. Biochem. 4*, 165-173.
Leatherbarrow, R. (1987) *Enzfitter*, Biosoft Hills Road, Cambridge.
Maniatis, T., Fritsch, E. F., & Sambrook, J. (1982) *Molecular Cloning: A Laboratory Manual*, Cold Spring Harbor Laboratory, Cold Spring Harbor, NY.
Mauguen, Y., Hartley, R. W., Dodson, E. J., Dodson, G. G., Bricogne, G., Chothia, C., & Jack, A. (1982) *Nature (London) 297*, 162-164.
Miller, J. H. (1972) *Experiments in Molecular Genetics*, Cold Spring Harbor Laboratory, Cold Spring Harbor, NY.
Mossakowska, D. E., Nyberg, K., & Fersht, A. R. (1989) *Biochemistry 28*, 3843-3850.
Neu, H., & Heppel, L. (1965) *J. Biol. Chem. 240*, 3685-3692.
Nishikawa, S., Morioka, H., Kim, H., Fuchimura, K., Tanaka, T., Uesugi, S., Hakoshima, T., Tomita, K., Ohtsuka, E., & Ikehara, M. (1987) *Biochemistry 26*, 8620-8624.
Oshima, T., Uenishi, N., & Imahori, K. (1976) *Anal. Biochem. 71*, 632-634.
Osterman, H. L., & Walz, F. G., Jr. (1978) *Biochemistry 17*, 4124-4130.
Quaas, R., McKeown, Y., Stanssens, P., Frank, R., Blöcker, H., & Hahn, U. (1988) *Eur. J. Biochem. 173*, 617-622.
Sanger, F., Nicklen, S., & Coulson, A. R. (1977) *Proc. Natl. Acad. Sci. U.S.A. 74*, 5463-5467.
Shirley, B. A., Stanssens, P., Steyaert, J., & Pace, C. N. (1989) *J. Biol. Chem. 264*, 11621-11625.
Stanssens, P., Opsomer, C., McKeown, Y. M., Kramer, W., Zabeau, M., & Fritz, H.-J. (1989) *Nucleic Acids Res. 17*, 4441-4454.
Sugio, S., Amisaki, T., Ohishi, H., & Tomita, K.-I. (1988) *J. Biochem. 103*, 354-366.
Takahashi, K. (1971) *J. Biochem. 70*, 945-960.
Takahashi, K. (1985) *J. Biochem. 98*, 815-817.
Takahashi, K., & Moore, S. (1982) *Enzymes (3rd Ed.) 15*, 435-467.
Tartof, K. D., & Hobbs, C. A. (1988) *Gene 67*, 169-182.
Vieira, J., & Messing, J. (1987) *Methods Enzymol. 153*, 3-11.
Wu, R., Wu, N.-H., Hanna, Z., Georges, F., & Narang, S. (1984) in *Oligonucleotide synthesis* (Gait, M. J., Ed.) pp 135-151, IRL Press, Oxford.
Zabinski, M., & Walz, F. G., Jr. (1976) *Arch. Biochem. Biophys. 175*, 558-564.
Zell, R., & Fritz, H.-J. (1987) *EMBO J. 6*, 1809-1815.

Purification and Spectral Study of a Microbial Fatty Acyltransferase: Activation by Limited Proteolysis†

Suzanne Hilton, William D. McCubbin,‡ Cyril M. Kay,‡ and J. Thomas Buckley*
Department of Biochemistry and Microbiology, University of Victoria, Box 1700, Victoria, BC V8W 2Y2, Canada, and Medical Research Council of Canada Group in Protein Structure and Function, Department of Biochemistry, University of Alberta, Edmonton, AB T6G 2H7, Canada

Received May 4, 1990; Revised Manuscript Received July 2, 1990

ABSTRACT: A fatty acyltransferase with a reaction mechanism similar to that of mammalian lecithin:cholesterol acyltransferase has been purified from culture supernatants of a mutant *Aeromonas salmonicida* containing the cloned *Aeromonas hydrophila* structural gene. Typically, more than 35 mg of protein were isolated from 2 L of culture supernatant. The amino-terminal sequence, amino acid composition, and molecular weight of the purified protein corresponded to predictions based on the sequence of the gene, indicating that the signal sequence had been correctly removed during export but that no further processing had occurred. Analysis of the far-UV circular dichroic (CD) spectrum of the enzyme showed that it consists of 31% α-helix, 21% β-sheet, and 16% β-turn, with 12% of aperiodic form. Treatment of the purified protein with a variety of proteases resulted in nicking near the C-terminus. This led to an increase in enzyme activity against lipids in erythrocyte membranes and increased rate of hydrolysis of *p*-nitrophenyl butyrate. Activation was accompanied by a change in the CD spectrum and a change in its aggregation state. The trypsin cut site was located between the two cysteines in the enzyme. Evidence is presented that the cysteines are joined by a disulfide bond and therefore cannot participate in acyl transfer. This may distinguish the microbial enzyme from lecithin:cholesterol acyltransferase. This is the second extracellular *A. hydrophila* protein that we have shown can be activated by proteolysis after it is released.

Esterases that catalyze the hydrolysis of lipids are found everywhere in nature. Recently they have attracted considerable attention, not only because of their important and essential roles in the metabolism of plasma and cellular lipids but because of potential biotechnological applications in medicine, food science, and synthetic chemistry (Harwood, 1989). *Vibrio* species release an unusual lipolytic enzyme (MacIntyre et al., 1979), which shares several properties with plasma lecithin:cholesterol acyltransferase (LCAT). Like LCAT, the microbial enzyme catalyzes the transfer of the sn-2 fatty acid of lecithin to cholesterol (MacIntyre & Buckley, 1978). Both the equatorial hydroxyl and the trans-fused A:B ring are required for optimal transfer to occur (Buckley, 1982).

† Supported by grants from the British Columbia Heart Foundation (J.T.B.), the National Science and Engineering Research Council (J.T.B.), the Alberta Heart and Stroke Foundation (C.M.K.), and the Mecial Researach Council of Canada (C.M.K.).
‡ University of Alberta.

0006-2960/90/0429-9072$02.50/0